APPLY DEM TO STUDY WET BINDER ADDITION AND DRY BINDER ADDITION WET GRANULATION IN A HIGH SHEAR GRANULATOR

By

SHENG-WEN CHEN

A thesis submitted to the

Graduate School-New Brunswick

Rutgers, The State University of New Jersey

In partial fulfillment of the requirements

For the degree of

Master of Science

Graduate Program in Chemical and Biochemical Engineering

Written under the direction of

Dr. Rohit Ramachandran

And approved by

_____

_____

_____

_____

New Brunswick, New Jersey

May, 2017

ABSTRACT OF THE THESIS

Applying DEM to study Wet Binder Addition (WBA) and Dry Binder Addition (DBA) Wet Granulation in a High Shear Granulator

by SHENG-WEN CHEN

Thesis Adivisor: Dr. Rohit Ramachandran

Wet granulation is widely used in many industries especially in the pharmaceutical industry for its capability to improve flowability and handling of powder substances. A discrete element model (DEM) was developed to study two kinds of liquid addition methods in wet granulation in high shear granulator: wet binder addition (WBA) and dry binder addition (DBA). To define the complex interaction in the systems, liquid bridge model and powder penetration theory are applied to develop the contact model. The DBA system possesses ten times higher viscosity particles than the WBA system. The results of two systems were compared and differences in viscosity profile were identified. Viscous regions are found to move when time progressing. The relationship between impeller and viscosity profile are studied. The great difference in viscosity is related to strong liquid bridge force and average bridge number in the DBA system. The strong liquid bridge force results in larger granules in the DBA system.

Acknowledgements

I would like to show my gratitude to Dr. Rohit Ramachandran for offering me the opportunity to join his research group and work with all brilliant people on interesting projects.

I want to thank Ashu Thamrakar for collaboration on the development of DEM model and support on the research. Without his help, I won't be able to make this thesis happen. I would also like to thank other members of the research group for providing suggestions on my work. Lastly, I want to thank my family and friends for supporting and encouraging me to make through the journey. I am blessed to have all of these great people in my life.

Table of contents

List of tables

List of figures

Chapter 1

Introduction and Objectives

1.1 Background of granulation

Wet granulation is an important process in many industries, such as mineral industry, pharmaceuticals, detergents, food, and chemicals etc. It's a particle enlargement process which is conducted normally by spraying binder solution to powder and sticking the particles together in order to form large granules [1]**.** By wet granulation, one can benefit from reducing dust, increasing in powder density. Besides, the properties of granules can be determined based on the binder and other materials which are involved in granulation. This makes it useful to decrease segregation and improve the flowability and handling of the powder. Furthermore, one can manipulate the dissolution, appearance, and compressibility of the product by choosing proper excipients and process variables. When developing low dose drug product, traditional direct compression will introduce unacceptable variability to product's content uniformity. Wet granulation is a good solution and can be performed in two ways, batch or continuous. There are several equipments that can conduct wet granulation; high shear mixer, fluidized bed, tumbling mixer and twin screw granulator are equipment commonly used.

However, the understanding of the wet granulation process is inadequate to its massive application. Throughout the past decades, researchers try to predict and control wet granulation behavior but it's still difficult to predict process performance of new formulation by their fundamental properties [2]. Although the task is still challenging, it has been approached by many ways. Starting from investigating how of material properties and process parameters affect product to now more attention are addressed to fundamental mechanism of granulation in microscopic aspect.

For process parameters, such as impeller speed, liquid flow rate, liquid addition method, and mixing time were studied [3]. For process design, determining the end point of wet granulation process is critical; thus, researchers developed methods such as the power consumption method and impeller torque method. Leuenberger et al. defined the power consumption profile of the process and pointed out that the plateau of power consumption curve would be the end point [4]**.** Rowe et al. discovered that the impeller torque changed due to the change in cohesive force between particles, which can be used to determine the end-point of the process [5]**.**

On the other hand, fundamental studies on the granulation process have been conducted throughout the years. Pioneering work done by Sastry et al. described the process by four mechanisms [6]**.** Later Litster et al. combined some of the mechanism and introduced new three mechanisms: Wetting and nucleation, Consolidation and growth, Attrition and breakage [7].

Wetting and nucleation is the first step of the formation of granules. The initial wetting of the binder fluid is meant to create nuclei from fine powder. The size distribution of nuclei will greatly influence the final granule size distribution. Wetting thermodynamics and kinetics of nucleation have been identified as key factors to nucleation. Hapgood et al. investigated the wetting properties of powder by the droplet penetration experiment [8]. By relating the ability of powder bed to absorb different kinds of droplet, they developed a method to quantify the wettability of the powder. Rowe et al. defined the spreading coefficient by the surface free energy of the material and related it to the kinetics of nucleation [9]. These works were combined into nucleation regime map by Lister and Hapgood [10]. They proposed that the interaction between drop penetrating time and dimensionless spray flux would determine the nucleation behavior. They divided nucleation into three regimes: drop-controlled regime, mechanical dispersion regime, and intermediate regime. Different regimes lead to different nucleation behaviors. Now one can predict and control nucleation by the nucleation regime map.

Consolidation is the compaction process that the internal liquid or air are squeezed out from the granules resulting change in porosity and liquid content on the surface. The effect of consolidation on granule yield strength was studied by Rumpf [11]. Ennis et al. implemented the viscous Stokes number to account for binder viscosity's effect. However, there has not been a model which could predict the extent of consolidation qualitatively yet [2]. The model takes capillary force, viscous force and friction force all into account will be a good approach to reach the goal and it is still an open region for development.

Growth behaviors of granules include coalescence and layering. Coalescence refers to two granules sticking together. Layering means fine powder accumulates on the surface of large granules. Normally, forces between two particles can be divided into two kinds of force: liquid bridge and inter-particle friction force. Liquid bridge force generated from the liquid bridge formed between wet particles. It consists capillary pressure and viscous force. Capillary pressure or static capillary force was calculated by Laplace-Young equation. Hotta et al. conducted an experiment and find the result agreed with the numerical results [12]. Lian et al. proposed gorge method to estimate the force [13]. Viscous force refers to the dynamics viscous bridge formed between particles which are approaching to each other. Adams et al. approached the viscous force by lubrication theory [14]. His work of viscous force was verified by Mazzone et al. [15] and Ennis et al. [16] in experiments. They showed that the viscous force will dominate in certain conditions.

While granule strength has been received extensive study, workers have tried to build up models to predict the strength. Rumpf proposed a model to predict the static tensile strength of a liquid bridge in granules. The model predicts the trend that granule strength will increase when the liquid surface tension or saturation increases [11]. However, the model does not include viscous force. Kapur et al. came up the model to describe the coalescence [17]. Ennis' model of the granule growth was extended by Liu et al. [18] [19]. However, a model which is able to simulate

all the interaction force including capillary force, viscous force and friction force is still a complex work. Another practical approach to predict granule growth behavior was proposed by Iveson, the growth regime map for nucleation [20]. By growth regime map, there is a potential for engineers to predict the granule growth based on two dimensionless groups, maximum pore saturation and the deformation number. This becomes valuable when dealing with a new formulation. Now one can know the growth behavior by doing less experiments. Scaling up can also be aided by the map.

The last mechanism is breakage and attrition. Breakage refers to the wet granules break into small pieces under shear force. Attrition or fracture means dry granules break down in the drying after the granulation or any process in sequence. Normally attrition generates dust which contradicts to the goal of the granulation. To avoid or reduce attrition is one of the aims of granulation control. Mostly the breakage shows its influence in intense agitation system such as a high shear mixer. Therefore, most of the studies focus on breakage in a high shear mixer or a tumbling mixer.

Breakage was identified through the addition of dye tracer to granulation [21]. In Ramaker's work, they applied dye pellets to granulation to study the equilibrium between breakage and growth [22]. They found an exponential relationship for the dye concentration in a size classes. The exponential rate constant was referred to the conversion rate constant. The smallest pellets had higher conversion rate constants. This indicates that small pellets are formed due to the breakage. Models have been developed to predict the breakage mechanism. Tardos et al. assume that granules will deform and break under shear stress if it exceeds the granule strength. They proposed a Stokes deformation number criteria to determine whether the breakage will take place [23].

The high shear mixer has been widely used in pharmaceutical industry since it has advantages in short processing time, less binder required compared to fluidized bed granulation, and the ability to handle highly cohesive material. Normally, there will be an impeller at the bottom of the bowl

like container in a high shear mixer. The particles will be loaded into the container and mixed by the impeller in the speed ranging from 50-100 rpm. There will also be a chopper on the side wall of the container, the purpose of it is to chop down the granules with too large size [1].

Traditionally, the granulation in a high shear mixer is wet binder addition (WBA). The binder solution is injected by a nozzle to the system. Another way of wet granulation in a high shear mixer is the dry binder addition method (DBA). Dry binder addition refers to the binder enters the system as dry solid particles instead of liquid state. Then the low viscosity liquid such as pure water is introduced to the blend and activates the binder. In the pharmaceutical industry, it is becoming increasingly popular to apply binder in a dry state in granulation [24]. Some researchers applied this method to study the dry binder properties' effect on granulation or mimic the melt granulation [25] [26]**.** They showed that dry binders can be activated if moisture makes the binder to drop below its glass transition temperature. This process is analogous to a melting binder. Kayrak-Talaya and Litster demonstrated that nucleation regime map can successfully predict the trend in dry binder system [27].

1.2 Mathematical techniques

As mentioned formerly, developing a model to predict granule growth is still difficult. However, researchers are making progress, especially in two areas: population balance models (PBMs) and discrete element modeling (DEM). PBMs are the models divide particles into groups based on their size and other properties such as porosity or liquid content etc. The models track the change in the groups of particles over time by solving the class of differential equations [28]. PBMs have been applied to simulate many particulate systems. Traditionally one-dimensional (1-D) PBMs are used to study the wet granulation process [29]; however, Iveson pointed out the limitations of 1-D PBMs to describe the system. The 1-D PBMs assume that conditions are uniform in the system which isn't true in a real case. As a result, multi-dimensional PBMs were proposed to account for the heterogeneities in the system [30]. The 3-D PBMs can simulate complicate

process but they are computationally intensive and apply many empirical correlations and parameters. Thus reduced order PBMs are developed to lower the computational load with minor accuracy loss [31].

In contrast to PBMs, DEM simulates the particle motion individually by solving the Newton's equation of motion. Thus, we can say that DEM is a more fundamental approach to study the powder behavior. To apply DEM, firstly one needs to build up the geometry of the system. Once the geometry is created, DEM will compute the particle motion by the contact model defined by the user. In every time step, the system detects the collision or contact based on the velocity and position profiles of the particles in the last time step. If there is a collision between particle and particle or particle and geometry, the contact model will be used to calculate the contact force between particles and geometry. Generally, two kinds of contact models are applied in DEM: the soft sphere model and the hard sphere model [32]. The hard sphere model assumes that the particles collided with each other instantaneously. The soft particle approach considers collisions as a continuous process that occurs over a period of time. In soft particle approach, the interactive forces are treated as continuous functions of the distance between particles [33]. Our group developed the new contact model based on the work of Remy's et al. [34]. This model computes a non-linear force based on Hertz-Mindlin contact model, which is a soft sphere model. The particle system in granulation has a large number of particles that most of the collisions occur simultaneously on one particle. Furthermore, in our system, there are multiple contact points in each granule. Therefore, it is rational especially in a cohesive particle system to apply a soft sphere model.

Particle-particle collision is detected when there is a large enough overlap between particles. That is, the distance between the centers of the particles is smaller than the sum of their radii. For collision between the particle and the geometry the case will be the distance between center of the particle and contact point is smaller than the radius of the particle. A tiny overlapped is

considered as deformation of the material. The details of how the model calculates the force will be mentioned in the experiment set up section.

Beside the contact force, DEM will take into account other body forces such as gravity to compute the total force applied to the individual particle.

$$\overrightarrow{F_T} = \overrightarrow{F_C^N} + \overrightarrow{F_C^T} + \overrightarrow{F_B} \quad (1)$$

$\overrightarrow{F_T}$ is the total force on the particle; $\overrightarrow{F_C^N}$ and $\overrightarrow{F_C^T}$ is the contact force in normal and tangential direction. And $\overrightarrow{F_B}$ is the body force which is gravity in our system. Total force is then used to calculate the acceleration of the particle by Newton's 2nd law (F=ma) and compute the new velocity and position profile.

DEM has been used to simulate the granulation due to its advantages of providing shear force and collision frequency of particles. Adams et al. applied DEM to study the mechanism of agglomerate coalescence and identified the effects of friction, viscous and capillary forces, pendular bridge rupture and particle elastic deformation on the process. Lian et al. continued the work by simulating the interaction of two-particle interaction and the impact coalescence between wet agglomerates [33]. Although DEM was firstly limited to a microscale study due to the intensively computational cost, there were studies try to simulate the on a larger scale. Gantt et al. utilized DEM to determine the coalescence kernel [35]. In this work, DEM showed a potential to provide information about collision frequency distribution, particle surface liquid, and relative velocities which are unknown in PBMs. Besides, DEM has been coupled with PBMs or computational fluid dynamics (CFD) to study powder behavior. Recently, Barrasso et al. built a two-way coupling system for a twin-screw granulator [36]. The PBMs compute changes in particle size distributions and properties, and DEM simulations are triggered when significant changes occur to calculate new correct collision and velocity data. And Sen et al. coupled it to a CFD model to simulate fluidized bed granulation [37]. However, these studies do not include the

liquid addition stage in the simulation which is an open area for investigation. In my study, I utilized DEM to study wet as well as dry binder addition wet granulation in a high shear mixer in liquid addition stage.

1.3 Motivation and objectives

As mentioned before, there are not many researches on the DBA system, especially applying DEM to study a DBA system. DBA is getting popular due to the simple operations in a manufacturing point of view. A pioneer PBMs work on a DBA system in our research group reveals that there are viscous regions in the system which acts differently to a WBA system. Granulator can be divided into the upper region and the lower region to develop a two-compartments PBMs. We assume that the upper region will be the viscous region since it's near the nozzle. This study meant to verify the assumption by extracting particle level information from DEM. The objectives of this study are listed below:

- Develop a customized DEM model to simulate WBA and DBA wet granulation in a high shear granulator.
- Identify the viscous regions in both systems and verify the assumption made in PBMs.
- Compare the WBA and DBA systems
- Extract particle level information for future DEM-PBM coupled framework

Chapter 2

Experiment set up and Model development

2.1 Materials and experiment

Our simulation mimics the granulation experiment conditions done by a research group in Bristol-Myers Squibb, New Brunswick, NJ, USA. In their experiment, microcrystalline cellulose (MCC), (FMC Co., Philadelphia, PA) was granulated with the binder in a 10-liter PMA high shear granulator. The binder used for this study was hydroxylpropyl cellulose (HPC EXF) obtained from Ashland Specialty Ingredients, Wilmington, DE. The total mass of the batch was 1,664 g with 96% of MCC and 4% HPC. Microcrystalline cellulose (MCC) is manufactured by acid hydrolysis of wood pulp or cotton. MCC is widely used in industries such as pharmacy, cosmetics or ceramics. Especially in the pharmaceutical application, MCC's properties such as inert chemical activity and absence of toxicity make it a common option for excipient [38]. HPC is a nonionic water-soluble cellulose ether prepared by reactions of alkali cellulose with propylene oxide at elevated temperatures and pressures. The ability to reduce surface tension in solution makes HPC a good candidate for the binder. In the case of wet binder addition, the binder solution is prepared by dissolving HPC in water. For dry binder addition, the binder particles were mixed with MCC before granulation, and water was added to the mixture during liquid addition stage. The operating conditions for the granulation experiment can be found in Table 2.1.

Parameter	Value
Mixing speed	306 rpm
Dry mixing time	4 min
Liquid spray rate	400 g/min
Liquid addition time	3 min
Wet massing time	15 min

Table 2.1: Experimental conditions for dry binder addition wet granulation in 10L high shear granulator

2.2 Scale-down of the system

Although DEM simulation can provide detail micro level particle collision information, it's computationally expensive. Therefore, to model a realistic system, DEM normally will be limited to a short time period. Due to the complicated particle interactions in the DBA system, we need to develop a customized contact model to describe it which makes the simulation will take more time to be completed. To make our simulation practical, scaling down the system must be considered. Enlarging the particles' radius to 2 mm, we scaled down the 10-liter system to 1 liter. Scaling of the high shear granulation had been investigated for many years. Cliff et al. proposed a scaling method by dimensionless group Power number and Reynolds number[39]. The Power number provides the relationship between drag force applying on the tips and the inertial stress. The Reynolds numbers relate the viscous force and the inertial force. Further extending the work of Cliff, Landin et al. take the Froude number into account which describes the balance between the centrifugal force and the gravity. The Froude number is given by [22] [40]**:**

$$Fr = \frac{DN^2}{g} \tag{2}$$

where D is the impeller diameter, N is the impeller speed and g is the gravitational acceleration. In a geometry similar system, the Froude number should be independent of scale. By maintaining the same Froude number, we obtain the same particle flow pattern in scaling. In addition to Froude numbers, there are other scaling methods such as constant impeller tip speed or relative swept volume [41]. All of these methods aim to maintain the similar force and flow profile of the system in the change of the scale. Beside the force and the flow profile, spraying is another key factor in the scaling. The change in spraying results in the change in binder dispersion leading to the change in nucleation. Nucleation is one of the mechanisms of the granulation. Therefore, keeping the spraying pattern the same will be crucial in scaling. Lister et al. points out that current scale-up strategy normally leads to poor liquid distribution. He proposed that the nucleation regime map can be a guidance in maintain the same spraying pattern. In the same materials case, the only variable in the nucleation regime map will be dimensionless spray flux ψ_a which is given by [42]:

$$\psi_a = \frac{3\dot{V}}{2\dot{A}d_d} \tag{3}$$

where $\dot{V}$ is the volumetric spray rate, $\dot{A}$ is the area flux which powder passing through the spray zone and d_d is the diameter of the droplet. To obtain the same spraying and nucleation, keeping the dimensionless spray flux is the way to scale down. In sum, for the flowing pattern we keep the Froude number constant and for the spraying pattern, we keep the dimensionless spray flux the same in our system. Since the volume of the system reduced from 10-liter to 1-liter, the length of the impeller reduced, too. To keep the Froude number the same, we can derive the equation [1]:

$$\frac{N_2}{N_1} = \sqrt{\frac{D_1}{D_2}} \tag{4}$$

where N_1 is the impeller speed of the system before scaled down, N_2 is the new impeller speed. D_1 is the length of the old impeller and D_2 is the new one. For dimensionless spray flux ψ_a, the

droplet diameter is the same after scale-down. We assume that the area flux $\dot{A}$ will be reduced by the square of the proportional of how the length decreasing in the scale-down. In order to reduce the computational time, we increased the volumetric flow rate by three times while keeping the liquid and solid ratio the same. This might cause the concern of the system moving into different regimes in the nucleation regime map. However, we assume that the drop penetration time is very small, the system will be still in the drop controlled regime after increasing the flow rate. Besides the flow and the spray pattern, the packing of the powder bed is another thing to be taken into account. That is, we kept the filling fraction the same during scale-down. Table 2.2 presents the variables changed in the scale-down.

	Original	Scale down
High shear granulator volume	10L	1L
Impeller length	110.00 mm	52.56 mm
Filling level	52.83 mm	25.25 mm
Total mass of the API and binder	1.664 kg	0.281 kg
Total number of the API and binder particle	32263	5457
Number of API particles	30623	5180
Number of binder particles	1642	278
Rotation speed of the impeller	306 rpm	443 rpm
Liquid addition rate	400 g/min	274.02 g/min
Liquid addition time	3 min.	44 sec.

Table 2.2: Operation variables change before and after scale-down.

2.3 Buildup of the geometry and the customized contact model

The geometry of the 1-liter high shear granulator is shown in figure 2.1 including an impeller and

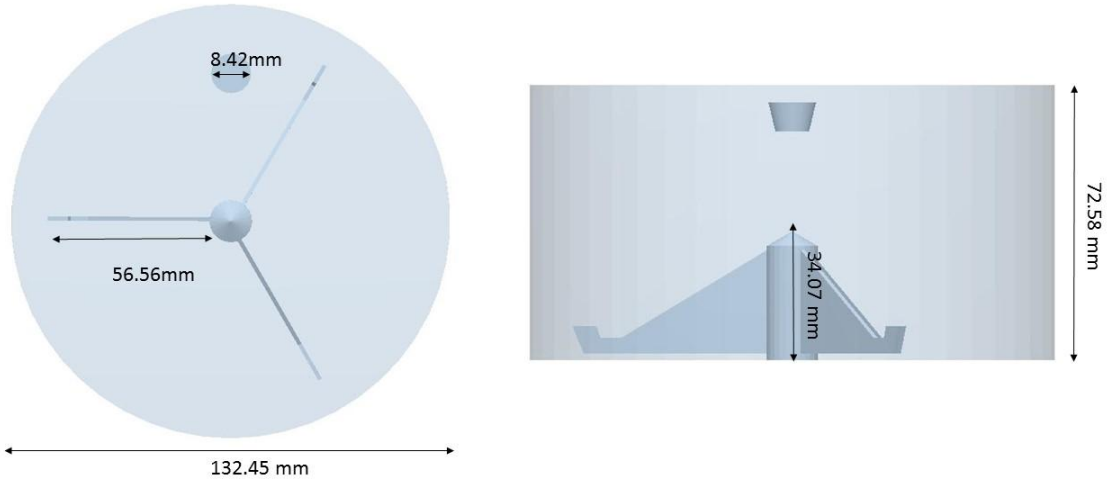

a nozzle on the top.

Figure 2.1: The geometry of the 1-liter high shear granulator.

Once we build our geometry of the system, the next step is to define the interactions between particles and droplets in the granulation. In WBA system, binder solution droplets and the MCC particles are the two elements. The combinations are quiet simple: liquid-liquid, liquid-API, API-API interaction. In the case of liquid meets liquid, the droplets will pass through each other and no transfer of any properties such as liquid or binder happen. However, the APIs shall bounce back as solid particles colliding with each other. In DBA system, combinations become more complex because there are three kinds of elements in the system now: binder particle, API particle and pure water droplet. Table 2.3 specifies the combinations of these elements.

Element	Element
Liquid droplet	Liquid droplet
Liquid droplet	Binder
Liquid droplet	API
API	Binder
API	API
Binder	Binder

Table 2.3: Combinations of interactions between different elements in a DBA system.

Interactions between elements must be defined. In liquid-liquid case, the droplets penetrate each other like in WBA system. Liquid-binder case, the binder will be dissolved by unsaturated droplets, shrinking in size. We assume that the binder dissolved gradually throughout the process. In another word, the concentration of the binder in a droplet will increase gradually up to saturated concentration when the droplet collides with a binder. For a liquid droplet meets an API, the API particle can absorb the droplet until reaching the maximum liquid retention of the API. Once it reaches the limit, the droplets won't be absorbed anymore and bounce back after the collision. In the collision between API and binder, the cases can be divided into two minor cases. One case is that the API possesses unsaturated liquid content which allows it to dissolve the binder. The other case is that API is saturated and won't be able to obtain any binder. When API meets another API, besides bouncing back like solid particles, liquid bridges will form if two wet particles are close enough to each other. The liquid bridge force is calculated based on the liquid bridge model which will be discussed later on. Binder-binder interaction is a simple one, they will bounce back like solid particles.

As mentioned before, the newton's motion law is applied to calculate the velocity and position profile of the next time step. The total force on a particle can be separated into three components:

contact force, cohesion force and body force. When the collision happens between elements or an element and the geometry, contact model should be applied to calculate the contact force. The force is divided into normal and tangential force. The model is modified from Tsuji et al. model which is developed based on Hertz-Mendilin contact model and possesses a Hook's simple linear spring and dashpot model [43]:

$$F_n = kx_n - \eta \frac{dx_n}{dt} \tag{5}$$

$$F_t = \begin{cases} kx_t - \eta \frac{dx_n}{dt} & if\ |F_t| \le \mu |F_n| \\ \mu |F_n| \frac{x_t}{|x_t|} & if\ |F_t| > \mu |F_n| \end{cases} \tag{6}$$

$$\eta = -2 \ln e \Big/ \sqrt{\pi^2 + (\ln e)^2} \tag{7}$$

where η is the damping coefficient, e the restitution, μ the friction coefficient. X_n the normal displacement, X_t the tangential displacement and k is the spring coefficient.

Cohesion force can be calculated by the liquid bridge force model in our system. It is noted that in our system, the particles are moving relatively to one another. Thus, the liquid bridge is not static. A dynamic bonding strength model should be utilized, in which the viscous force will be taken into account. The dimensionless group capillary number *Ca* can be used to determine whether the system is capillary force dominating or intermediate system [16]:

$$Ca = \mu U / \gamma \tag{8}$$

where μ is the viscosity, U is the particle relative velocity and γ is the surface tension. In a DBA system, the binder dissolving process will generate the viscous solution which makes *Ca* go into the viscous effect dominating regime. Since the work of Remy et al. study the system in capillary component only, we need to take into account the viscous component in our work[34]. We

classified the situations into two cases: *Ca* < 0.001 and *Ca*>0.001. For *Ca* < 0.001 which happens in the early stage of the process, the capillary force dominates in the case ($F = F_{cap}$). In another case, when *Ca* becomes larger than 0.001 due to the dissolution of the binder, the viscous force will dominate in the liquid bridge model ($F = F_{cap} + F_{vis}$). The capillary force between particles can be computed as [13] [33] [44] [45] [46] [47] :

$$F_{cap}^{p-p} = \frac{4\pi\bar{r}\gamma\cos\theta}{1+\frac{1}{\sqrt{\frac{1}{1+\frac{V_{liq}}{\pi\bar{r}S^2}}}-1}} \tag{9}$$

$$\bar{r} = \frac{r_i r_j}{r_i + r_j} \tag{10}$$

For the capillary force between particle and a wall, it will be:

$$F_{cap}^{p-w} = \frac{4\pi r\gamma\cos\theta}{1+\frac{S}{\sqrt{\frac{\pi r_i}{V_{liq}}}}} \tag{11}$$

V_{liq} is the volume of the liquid involved in the liquid bridge. S is the distance between two objects (particle or wall). r_i, r_j are the radius of the particles involved in the contact. θ is the contact angle of the particle. One needs to note that minimum separation distance S_{min} needs to be set to avoid the force going into infinity when two objects attached to each other ($S = 0$) [48]. S_{min} will be determined by roughness of the particle which we set to 10^{-6} m in our work. Shi and McCarthy proposed an equation to calculate the volume of the liquid bridge contributed from particle i [49]:

$$V_i = \frac{L_i}{2} \times \left(1 - \sqrt{1 - \frac{r_j^2}{(r_i + r_j)^2}}\right) \tag{12}$$

L_i is the total liquid volume on particle i. For another particle j involved in the liquid bridge, the contribution to the liquid bridge volume will be

$$V_i = \frac{L_j}{2} \times \left(1 - \sqrt{1 - \frac{r_i^2}{(r_i + r_j)^2}}\right) \tag{13}$$

The total volume of liquid bridge will be

$$V_{liq} = V_i + V_j \tag{14}$$

A liquid bridge is destroyed when the distance between objects is larger than critical rupture distance *Sc*. Lian et al. proposed an equation to estimate the critical rupture distance by solid-liquid contact angle θ and liquid bridge volume V_{liq}. The equation applies to either particle to particle or particle to wall [13]:

$$S_c = (1 + 0.5\theta)V_{liq}^{\frac{1}{3}} \tag{15}$$

As mentioned before, viscous force dominates when capillary number *Ca* is larger than 0.001. It can be divided into normal and tangential viscous force which are:

$$F_{vis} = F_{vis}^n + F_{vis}^t \tag{16}$$

The normal viscous force is derived from the Reynolds lubrication theory [33]:

$$F_{vis}^n = \frac{6\pi\mu R^* v_r^n R^*}{S} \tag{17}$$

$$\frac{1}{R^*} = \frac{1}{R_1} + \frac{1}{R_2} \tag{18}$$

where μ is the viscosity, v_r^n is the relative normal velocity between two spheres, R^* is the reduced radius calculated by radii of the two spheres.

For tangential viscous force, there are no many studies. However, Goldman et al. approached the force by studying the motion of a rigid sphere to a rigid wall with semi-infinity viscous fluid between the sphere and the wall. If the distance between the wall and the sphere is very small, they compute the viscous force with an analytical solution as the following [50]:

$$F_{vis}^{t} = (\frac{8}{15}\ln\frac{R}{S} + 0.9588)6\pi\mu R v_r^t \quad (19)$$

where v_r^t is the relative tangential velocity, R is the radius of sphere (particle). In the case of particle to particle interaction R should be replaced by reduced sphere radius R^*.

In the wet binder addition granulation, the binder solution is fixed concentration. However, in a dry binder addition granulation, the concentration of the binder solution keeps changing through the process due to the dissolution of the binder. The change in concentration will result in a change in viscosity and surface tension of the binder solution. In liquid bridge model, the viscosity and surface tension are critical variables. Not only do them determine the capillary number *Ca* but also appear in the equation of the capillary force. Another thing needs to be noted is that when a binder solution droplet meets an API particle, the droplet will start to penetrate into the pores of the particle. This leads to the change of the external liquid (liquid on the API particle surface) which is used to form the liquid bridge. Since the volume liquid bridge is an important variable in the liquid bridge model, the change in volume of liquid bridge also influences the granulation. How does the dissolution of the binder impact the process is illustrated by the figure 2.2.

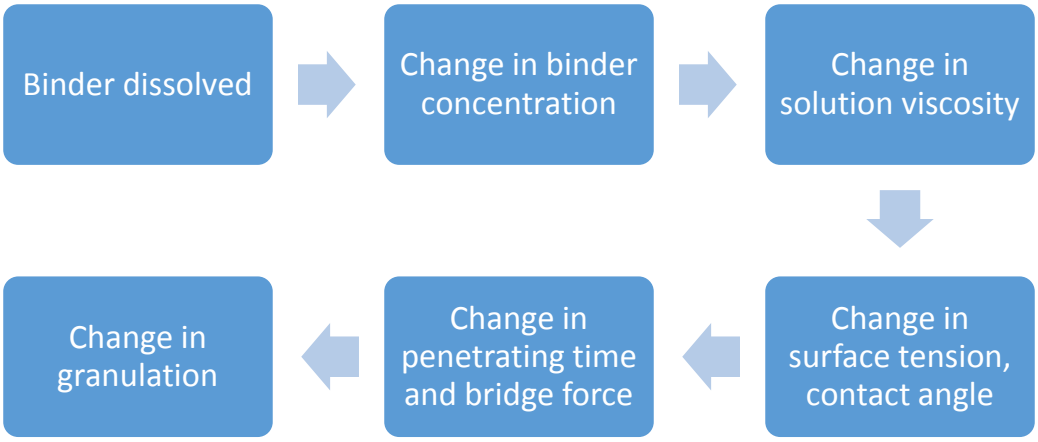

Figure 2.2: The flow sheet of how dissolution of the binder impacts the granulation.

To determine the dissolution model of the binder, we assume that it is a fast process which the droplet reaches maximum concentration in a second. When a saturated droplet meets a pure water droplet, it will be diluted and be able to dissolve the binder again. Applying such mechanism we can obtain the instant concentration of every droplet. We determine the viscosity of the binder solution according to the instant viscosity and the external liquid content. The relations between concentration, viscosity and surface tension of hydroxylpropyl cellulose had been studied in many papers [51] [52] [53] [54]. By doing the regression of these data, we obtained equations to calculate viscosity and surface tension from the concentration. Feeding updated data to the model to gain the capillary number and the liquid bridge force.

It's essential to track the external liquid content of API particles to compute the volume of the liquid bridge. Besides the work of Hapgood et al. [8], to define the mass of liquid penetrating into a porous powder bed, Siebold et al derived an equation from Washburn equation [55]:

$$w^2 = c\frac{\rho^2\gamma\cos\theta}{2\mu}t \tag{20}$$

where *w* is the weight of liquid penetrating into the pores, *c* is the geometric factor and is constant if the packing of the bed and particle size remains the same. ρ is the density of the liquid which we assume to be constant, and *t* is the time period of observation. In our study, we assume that when a drop meets an API particle, the way of penetration is just like the liquid going into the powder bed case. We also assume that the saturated binder solution will penetrate into the pores and reach the maximum internal liquid content after about 7.5 seconds if there is enough external liquid content. The maximum internal liquid content is obtained from the work of Luukkonen's et al.[56]. Plugging the maximum internal liquid content and other variables into the equation, one can derive the geometric constant *c*. With geometric constant, we can determine the internal liquid content for every particle in each time step.

The next step of the setup of the simulation is to plug in material properties and determine the input variables of the simulator. Those variables are listed in Table 2.4. The simulation starts with the settling down all solid particles which takes 0.2 seconds. The solid particles are generated randomly in the system to avoid segregation between binder and API particles. After the particles settle down, the impeller is activated. By checking if the average velocity of the particles is reaching steady state, we start the liquid addition at 2 seconds. The spraying continues throughout the whole simulation for 42 seconds and stops when the all the liquid amount is introduced to the system. Two simulations are performed on a 30 cores in an Intel Xeon ® CPU@ 2.40 GHz with 64 GB RAM Dell Precision Tower 7810 workstation. Each simulation takes 15 days to simulate 44 seconds.

API		**Binder**	
Particle Radius	2 mm	Particle Radius	2 mm
Density	1557 kg/m^3	Density	1210 kg/m^3
Porosity	10 %	Washburn Constant	3.65E-17
Washburn Constant	3.65E-17	Poisson's ratio	0.33
Maximum liquid retention	0.45 kg/kg	Shear Modulus	1E6 Pa
Poisson's ratio	0.3	**System**	
Shear Modulus	1E6 Pa	Time step	2.70734e-06 s
Coefficient of Restitution	0.575	Total time	44 s
Coefficient of Static Friction	0.176	Mesh size	4 mm
Coefficient of Rolling Friction	0.01		
Droplet (WBA)		**Droplet (DBA)**	
Particle Radius	1 mm	Particle Radius	1 mm
Density	1000 kg/m^3	Density	1000 kg/m^3
Washburn Constant	3.65E-17	Washburn Constant	3.65E-17
Poisson's ratio	0.25	Poisson's ratio	0.25
Shear Modulus	1E8 Pa	Shear Modulus	1E8 Pa
Fluid Concentration	5.547 wt%	Fluid Concentration	0 wt%
Contact Angle	1.04877 rad	Contact Angle	1.0486 rad
Surface Tension	0.0410319	Surface Tension	0.0741
Solubility	12 %	Solubility	12 %
Washburn Constant	3.65E-17	Washburn Constant	3.65E-17

Table 2.4: Input variables for the DEM simulation.

Chapter 3

Results and Discussion

In my study, I focus on the comparison between WBA and DBA system. In the following I will compare the data extracted from the DEM simulation and discuss the trends in the figures.

3.1 Viscosity differences between two systems

In figure 3.1, the API particles are colored based on the viscosity of the liquid in the particles. The deeper the blue is in particles indicates a higher viscosity. In both systems, the particles increased in viscosity when the nozzle introduced the liquid into the system. In the WBA system, the upper region received more binder solution and turned into blue in the early stage of granulation (time=10 sec.) Since the binder solution in the WBA system is fixed to 5.547%, the concentration of binder in the API particles can only be two levels: 0% or 5.547%. Thus API particles are only in two kinds of colors, white and blue (Dark cyan particles are droplets in the system). However, on the left-hand side in figure 3.1, the cyan color and the red color appear in the DBA system. Red particles are binder particles (HPC EXF) and cyan color indicates that there is an intermediate level of binder concentration in API particles. Besides the third color in the system, there is another difference between two systems at 10 seconds: the distribution of the viscous (blue) particles in the system. From the side view, we can see that the viscous particles do not group up in the upper region but appear around the binder (red) particles in the DBA system. This is because that the API particles obtain viscosity in two kinds of interactions between particles: API-droplet and API-binder interactions. In the API-droplet case, if an API meets a droplet with some binders in it, the API absorb the droplet and gain binders. In the API-binder case, the API can dissolve binder if there is unsaturated external liquid in the API. The distribution of solid binders and the position of the nozzle determine the viscous regions in the

DBA system in the early stage. In the middle stage of granulation (time= 20 seconds), some particles remain low viscosity in the WBA system. However, there are more particles remaining low viscosity in the upper region of the DBA system. In the end of the liquid addition (time= 40 seconds), almost all the API particles in both systems become blue indicating that the system is reaching homogenous state. Besides this, the accumulation of droplets is observed in the figure. Based on our experiment conditions, the liquid amount we put in the system is more than the amount that API particles can absorb. There are some binder particles remain undissolved in the end of the granulation in the DBA system. Although two systems possess the same ratio of binders to API particles, the undissolved binder particles in the DBA system means that the concentration of the binder in the API particles will not be the same as in WBA system. One needs to note that these observed difference should be further investigated since the side view of the simulation only reveal part of the system. A quantitative analysis should be carried out to verify the differences.

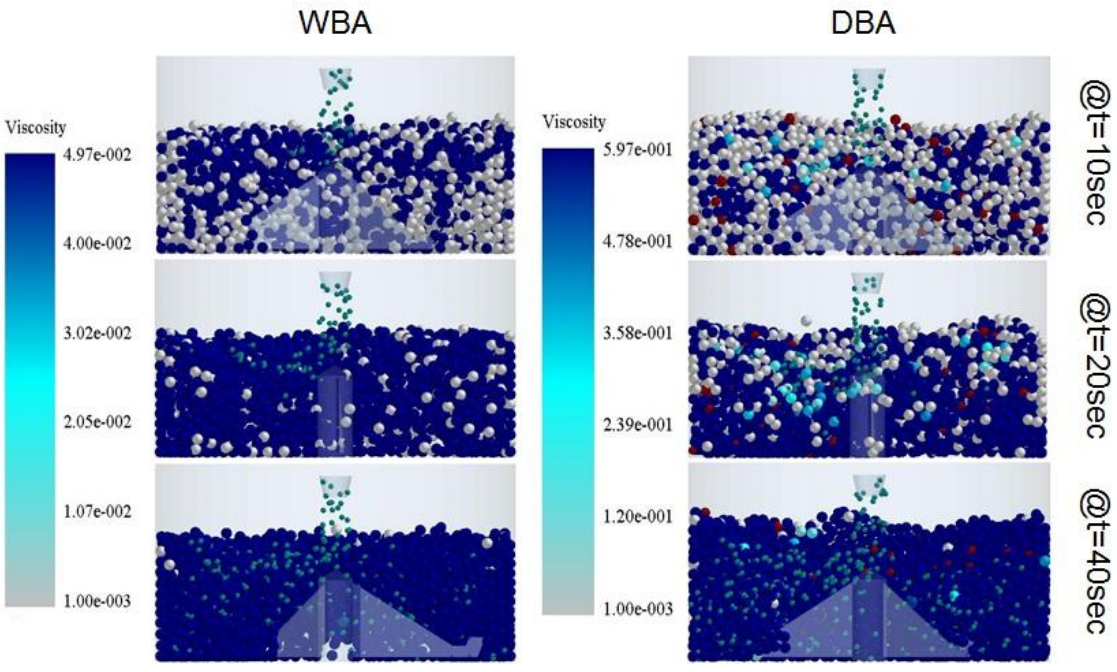

Figure 3.1: The viscosity change of the particles in WBA and DBA system. (Dark cyan particles are droplets and the red particles in the right are binder particles (HPC EXF))

To analyze the system quantitatively, I post-processed the data extracted from DEM simulation with MATLAB software. In figure 3.2, the total mass of binder solid particles is normalized by dividing it to the total mass of the binder before the liquid was added. Binder particles are losing mass due to the dissolution and 10% of them remain undissolved at the end of the simulation. These particles are supposed to be dissolved in a longer period of mixing since there are droplets accumulating in the system. The accumulation of the droplets in the system is also supported by the liquid content curve in the API particles. The absorption of the liquid in API particles slows down at 25 seconds and almost reaches maximum liquid retention in the end of the liquid addition. The saturation of the liquid in the pores of API particles is also verified by the internal liquid content curve, it reaches 10% in the end which is the porosity of the API.

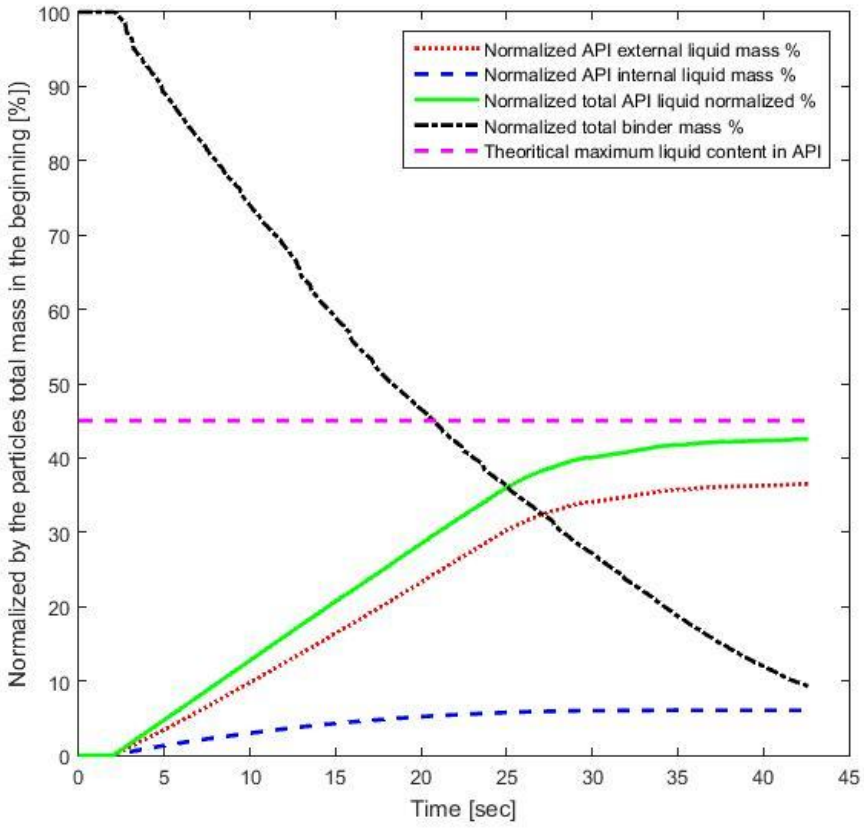

Figure 3.2: The liquid content and binder dissolution curves in DBA system.

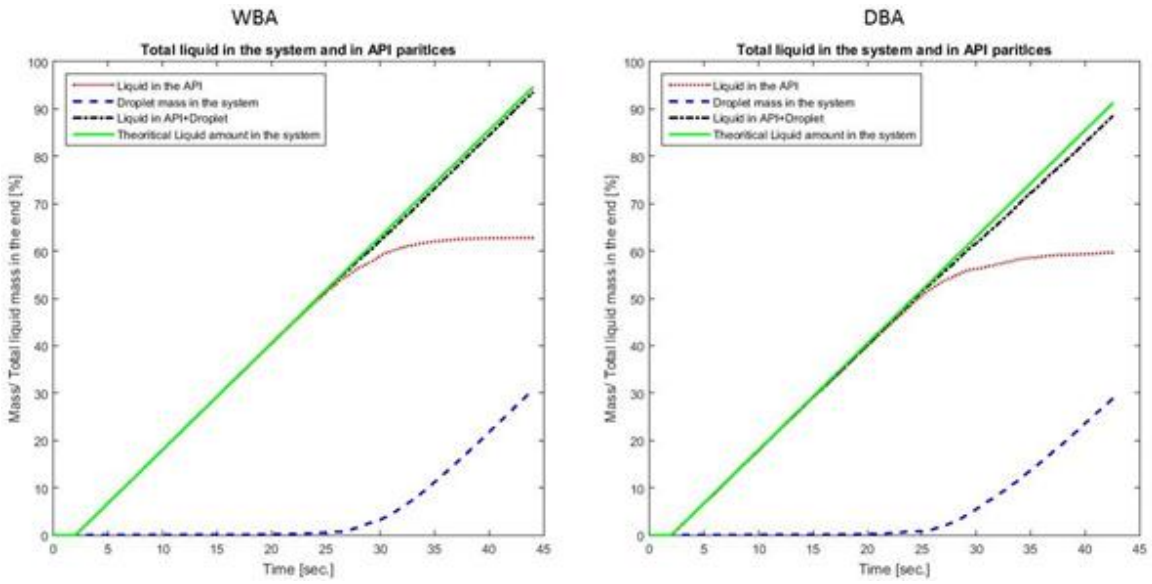

Figure 3.3: Liquid content in both systems. Different kinds of liquid content are normalized by theoretical total liquid amount in the system.

Furthermore in figure 3.3, we can see that in both systems, droplets start to accumulate in the system after 25 seconds.

To study the viscous regions in the systems, I classify API particles into two kinds of particles: low viscosity and high viscosity particle. Since the maximum binder concentration in the API is 12%, the maximum viscosity will be 0.059 Pa.s. For API with viscosity more than 0.02 Pa.s, it is classified as high viscosity. Figure 3.4 presents the growth in percentages of high and low viscosity particles. API in both systems turn into high viscous particles after the liquid addition.

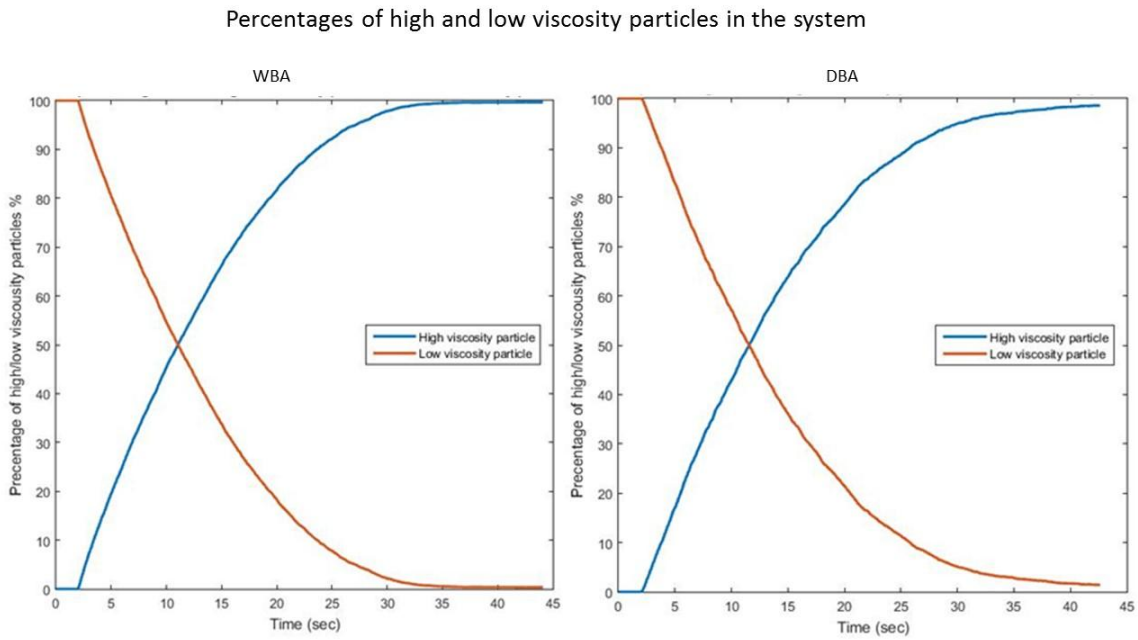

Figure 3.4: Percentages of high/low viscosity in the system. (Particle number/Total particle number)

However, in figure 3.1, the average viscosity of high viscosity particles are different in two systems. In the WBA system, high viscosity particles have viscosity around 0.05 Pa.s. And in the DBA system, it's around 0.59 Pa.s which is ten times more than the WBA system. Although we put in the same ratio binder and API in two systems, due to the difference in liquid addition methods, the DBA system has higher viscosity. The interactions between API and binder lead to the high viscosity in the DBA system. For example, a clean API particle (without any binder and liquid) colliding with a small pure water droplet. The API particle then collides with a binder and become saturated in binder concentration. Once the binder is absorbed by the API, there is no way that it can get out of the API. Thus the API might get diluted when it collide to another water droplet. However, It will become saturated again when it touch another binder particle and stay in contact for enough long time. In the end, all the high viscosity API particles obtain maximum concentration of binder in the DBA system and lead to high viscosity in the system. In the WBA system, the binder is added to the system in fixed concentration of the solution, there is no chance for API to obtain additional binder.

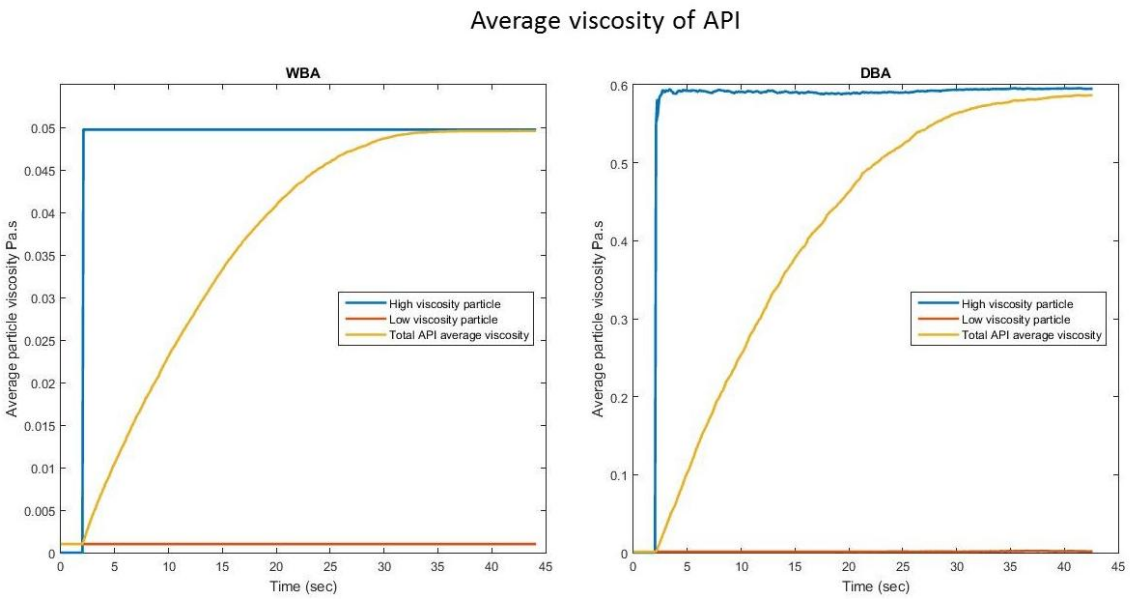

Figure 3.5: Average viscosity of high/low viscosity particles in two systems.

In figure 3.1, we observed that there are viscous regions in the systems. For the WBA system, the upper region seems to be more viscous in the early stage (time= 10 seconds). For the DBA system, there are more high viscosity particles in the lower part of the granulation in the middle of the liquid addition (time= 20 seconds). To check if the trend is true, viscosity profiles of two systems in height direction and radial axis are plotted in figure 3.6 and figure 3.7. Both trends are confirmed by the figures. In the WBA system, at 5 and 10 seconds, the average viscosity of the particles is high in the upper region. In the DBA system, the lower part of mixer possesses high average viscosity at 20 seconds. For the WBA system, since APIs get the binder solution from the nozzle on the top of the mixer, they turned into high viscous particles in the upper region. For DBA system, the trend we observed is contradicted to the pioneer PBM work in our research group. In PBMs work, we assume the viscous region in the DBA system will be at the upper 30 % height in the system like the case in WBA system. However, the viscous region seems to locate in the bottom of the granulator in DEM simulation. The explanation of the contradiction might be the impeller in the bottom of the granulator improves the mixing in the region. The better mixing increased the contacts between all kinds of particles and leads to higher viscosity. However,

additional experiments such as changes in impeller design or speed are needed to be conducted to justify the explanation.

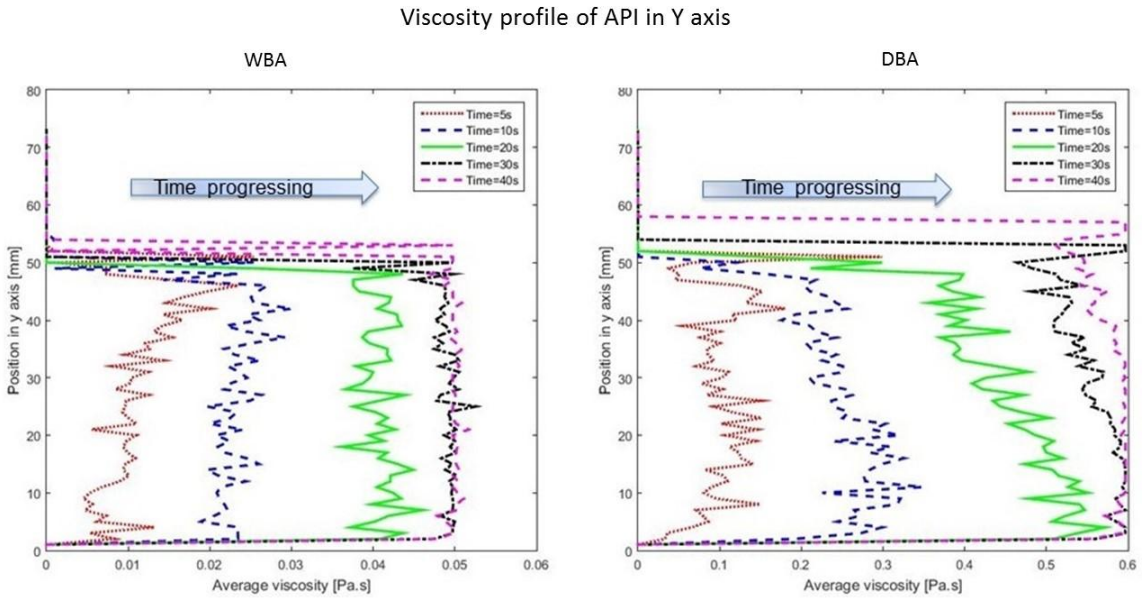

Figure 3.6: The average viscosity of API verse height (The viscosity of the APIs in the same height is averaged out).

In figure 3.7, one can see that the impeller influences the locations of the low viscosity regions. In the regions which are away from the impeller, the viscosity drops down greatly. Besides the impeller, the nozzle position is also crucial to the viscosity profile in the early stage. In the positions right below the nozzle (gray square on the top of figure 3.7), the viscosity is the highest. The influence of the impeller on system is supported by figure 3.8. The shrink in size of binder in figure 3.8 means the dissolution of the binders. From the locations of small binder particles, we can tell that in the inner circle close to center the number and size of binder decreased greatly. However, in the outer circle region close to the wall of granulator, there are still binder particles with the original size at the end of simulation. The difference in size of binder supports the effect of the impeller.

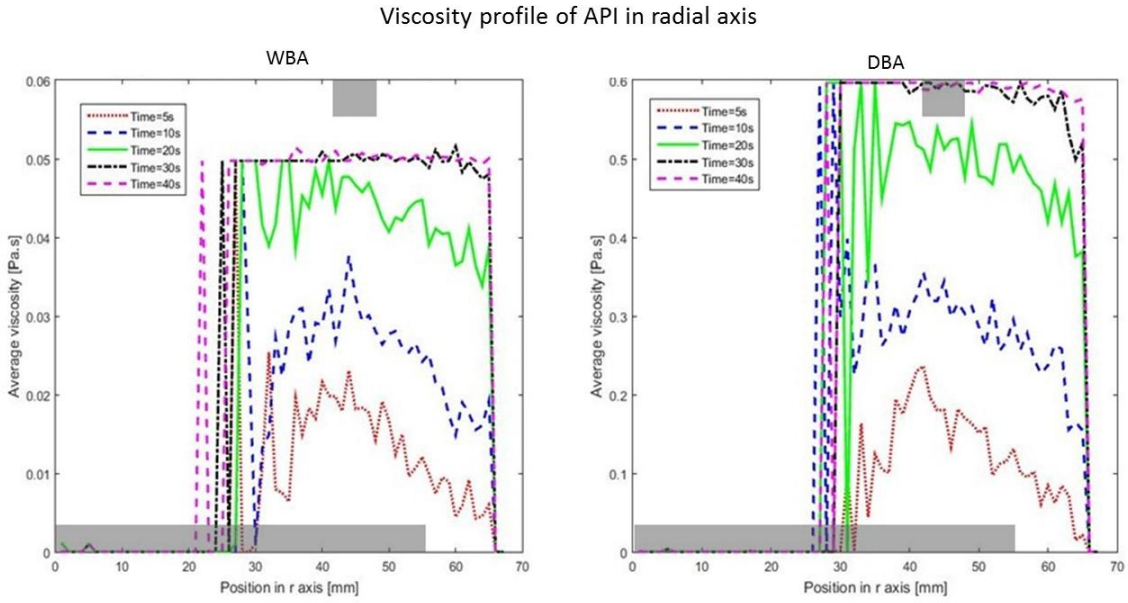

Figure 3.7: The average viscosity of API verse the distance of particles to center (The viscosity of the APIs in the distance to center is averaged out). The gray square on the top indicates the position of nozzle. The gray rectangle in the bottom indicates the length of the impeller.

3.2 Average velocity of the API particles

Next, I compared the average velocity of high/low viscosity particles in two systems. For high viscosity particles, two systems share a similar trend and magnitude. However, for low viscosity particles, the average velocity starts to decrease at the late stage of the simulation. By checking the velocity of individual low viscosity particle, I hypothesize that the low viscosity particles in the late stage are in the dead zone of the granulator. In figure 3.9, most of the low viscosity particles in the WBA system after 20 seconds are at the height around 2~6 mm which is in the gap between the blade and the bottom of the granulator. Further taking a look into the velocity profile of the particles in figure 3.10, low velocity zones are observed in the rim of the vessel. Therefore, the drop of velocity in low viscosity particles remains one more thing to be explained: why does the dead zone in the DBA system not create the drop in average velocity of low viscosity particle. I believe that the particles in the DBA system possess stronger liquid bridges

between particles. This helps the particles in dead zones be dragged out from the zones by other moving particles. By checking the individual particle information, low viscosity particles in the DBA system are found with height 65~70 mm. This indicates that the dead zones in the DBA system don't affect particle velocity much.

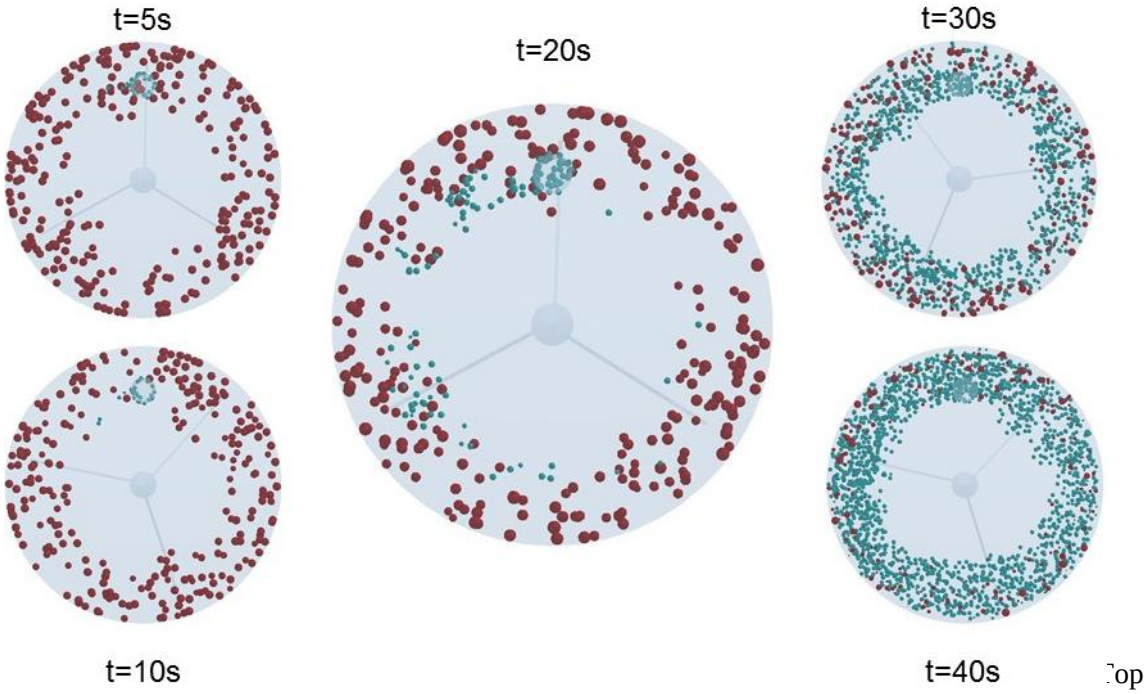

Figure 3.8: Top views of the DBA system at different time. Red particles are binders and dark cyan particles are droplets.

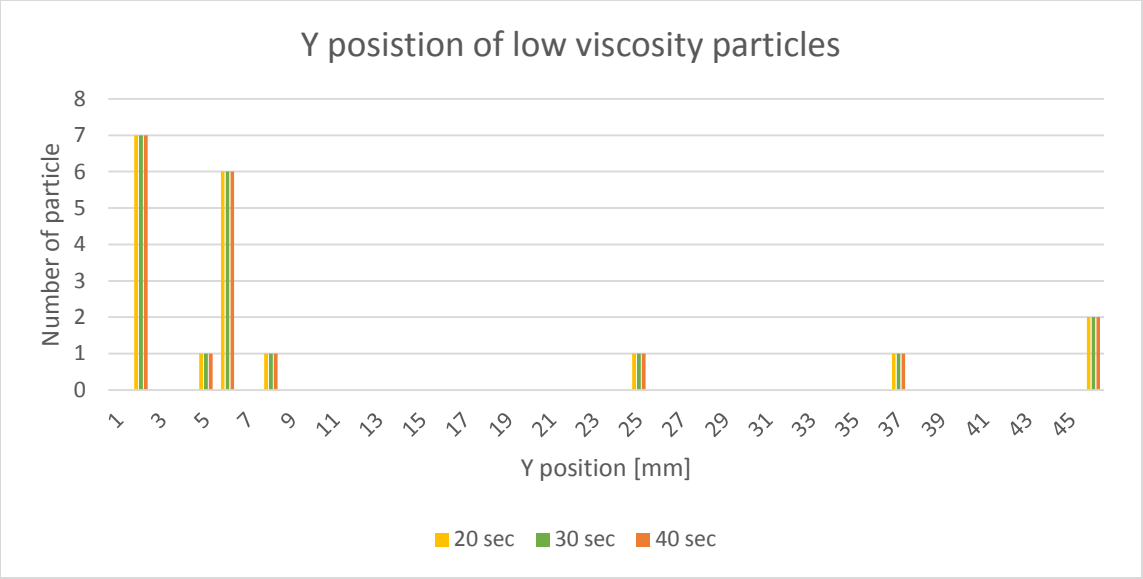

Figure 3.9: The height of individual low viscosity particles in WBA system at 20, 30, and 40 seconds.

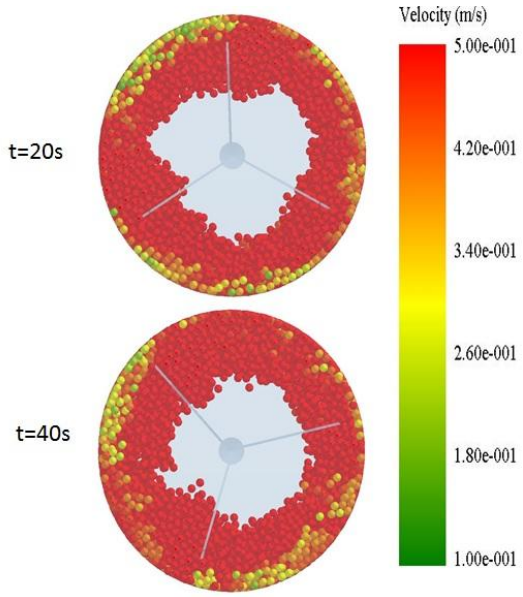

Figure 3.10: velocity profile of the API particles in WBA system (Pictures are taken from the bottom of the granulator)

3.3 Capillary number *Ca* and liquid bridge number

Figure 3.11 supports our assumption made in model development. Both systems go into the viscous force dominating regime ($Ca > 0.001$) after the liquid addition starts. Due to the viscous system in the DBA system, we can see that the capillary number of it is 100 times larger than the WBA system. The difference in viscosity will impact the liquid bridge forces in the systems. Figure 3.12 shows that the liquid bridge force in the DBA system is 5 times stronger than the WBA system. The bridge force in both systems start to decrease after 25 seconds.

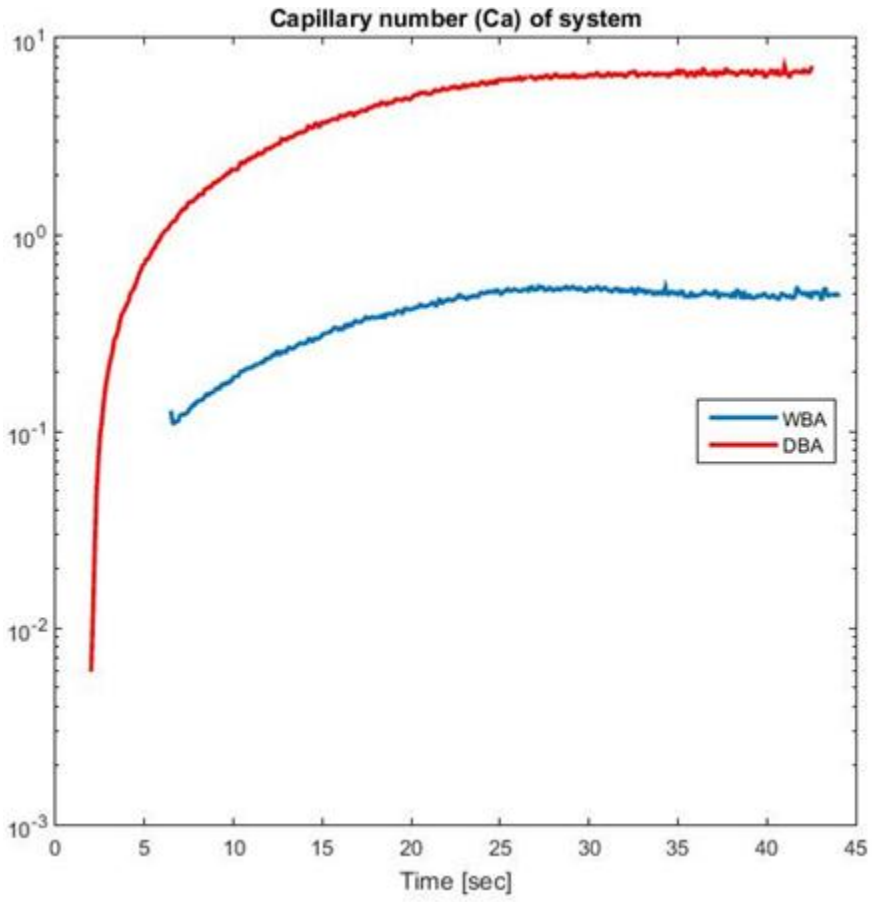

Figure 3.11: Capillary number *Ca* in both systems.

The explanation might the accumulation of the droplets in the systems. After the droplets accumulate in the system, it share the space to form the liquid bridge between APIs. That is, the

droplet might force the API particles form a liquid bridge in larger separation distance results in a weaker liquid bridge.

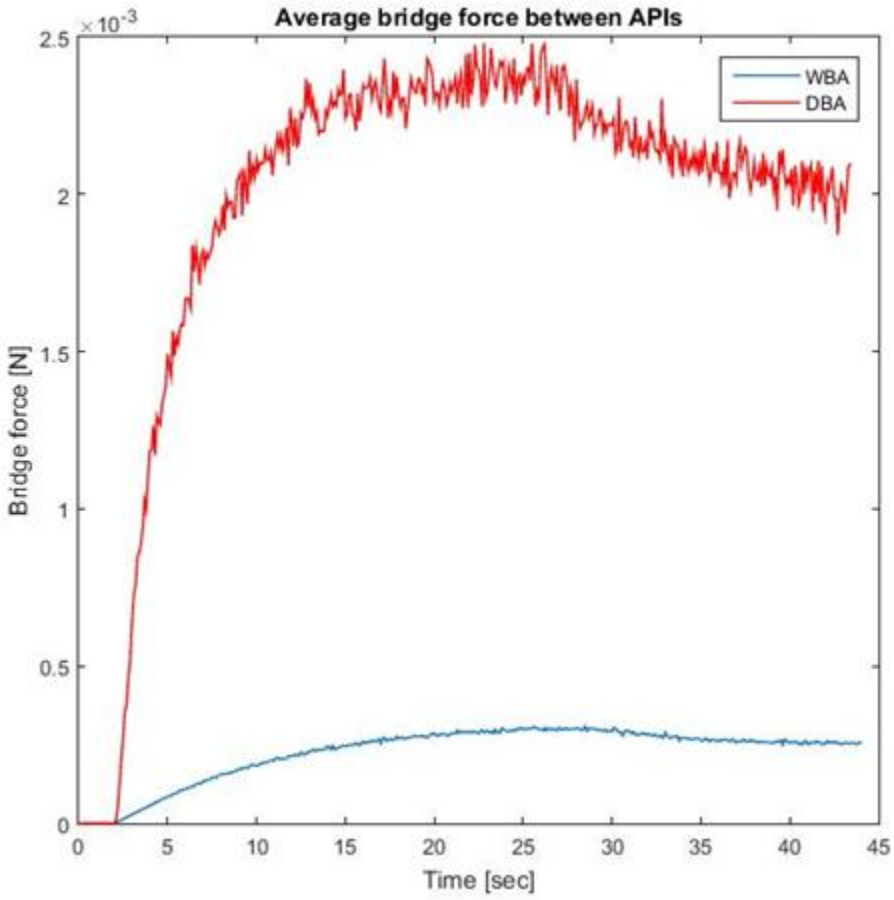

Figure 3.12: Average bridge force of the APIs in two systems.

3.4 Collision frequency and granule size

Collision frequency is an important input variable in PBMs. Higher collision frequency will facilitate coalescence mechanism in granulation [35]. In our system, collision frequency is calculated by dividing the total collision number between APIs by the DEM time step. In figure (collision frequency), the WBA system has slightly higher collision frequency than the DBA system in high viscosity particles. I hypothesize that in the DBA system the stronger liquid bridges hold the particles together in motion. Since the particles move together, the collision

frequency might reduce as a result. In WBA systems, the weaker liquid bridge force leads to smaller granules formation and higher collision frequency.

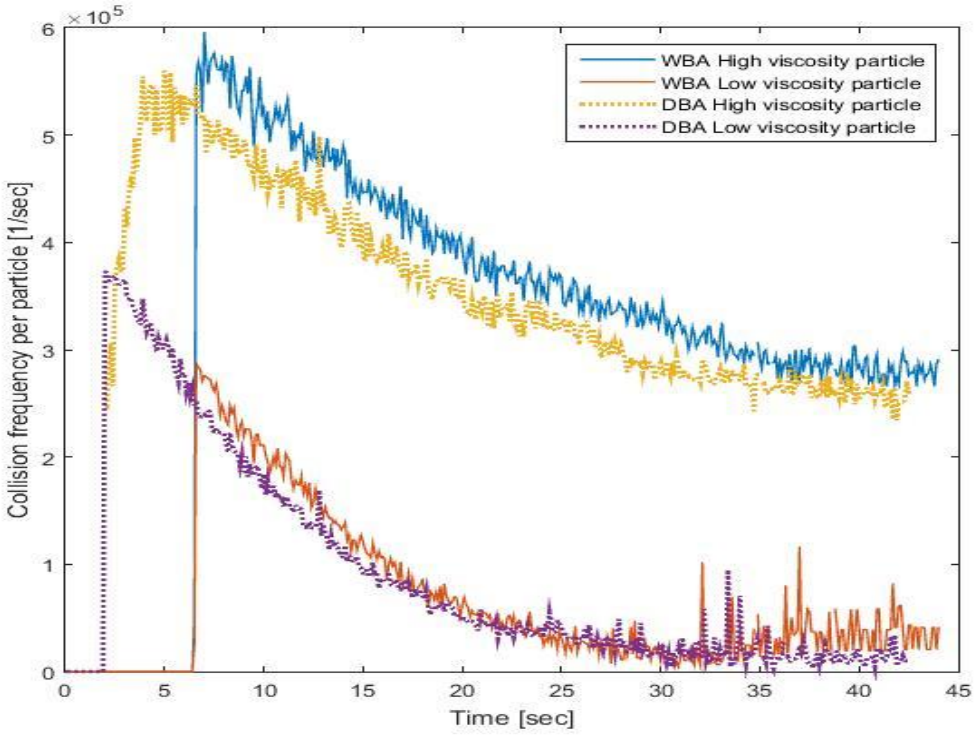

Figure 3.13: Collision frequency of the high/low viscosity particles in both systems.

In a DEM simulation, it's hard to describe the size of granules since all the particles are tracked individually. However, the average number of liquid bridges on one API particle can be an indicator to the size of granules in the system. In figure 3.14, the DBA system has higher average bridge number than the WBA systems. This indicates that the granule size in the DBA system is larger than the WBA system. The reason lays in the fact that high viscosity in DBA system forms strong liquid bridges between particles that can resist shear forces. Effects of viscosity on granule size in a high shear mixer or fluidized bed are reported in the literature [2][57]**.** However, if we want to justify the explanation, we will need PBMs to actually compute the particle size distribution.

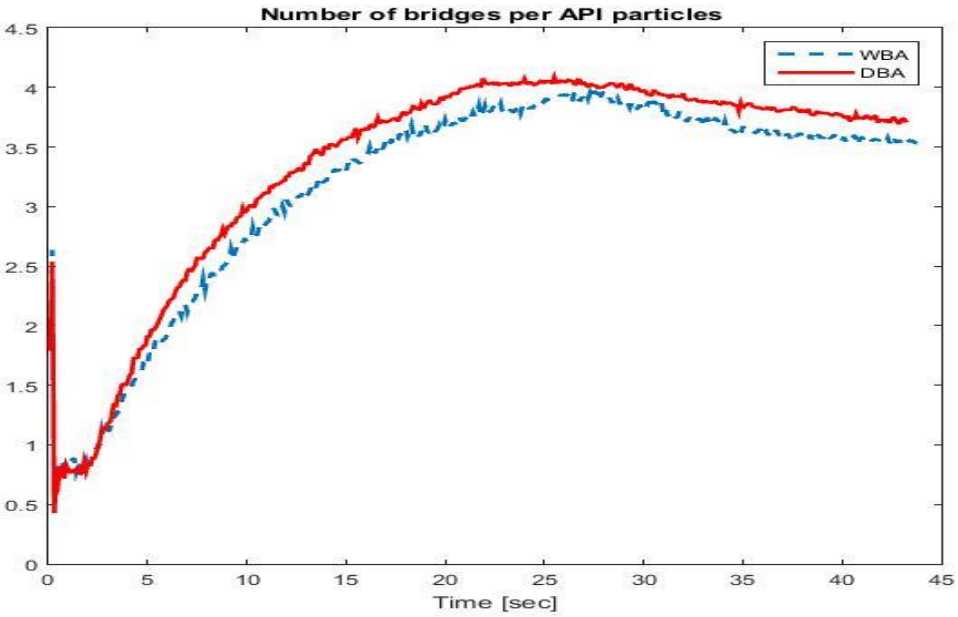

Figure 3.14: Average number of liquid bridges in one API particle.

Chapter 4

Conclusion and Future work

A mathematical model was developed for a 1-liter high shear mixer based on DEM methodology. A customized contact model was built to define the interactions between particles in a WBA and a DBA wet granulation. The simulation results were extracted and post-processed with the software, MATLAB. A great difference in viscosity between two systems is observed. Viscous regions are found distributed differently in two systems. In the early stage of granulation (2~10 seconds), both systems have viscous regions in the upper region of the granulator because the locations are near the nozzle. However, in the middle of the granulation (10~30 seconds), viscous region moves to the lower region of the granulator. The reason might be the mixing around the impeller is better compared to the upper region. The improvement in mixing increases the contacts between API, droplets, and binder. Therefore the concentration of binder increasing in the API results in the high viscosity in the lower region. In radial axis, low viscosity regions are found in the outer circle of the granulator in both systems. The impeller once again contributes to the viscosity profile. The shrink of the binder in figure 3.8 supports the reasoning. Nevertheless, the motion viscous regions suggest that it's better to track the locations of viscous region dynamically than simply divide the regions into upper and lower regions. Dead zones are identified in the gap between the impeller and the bottom of the granulator in the WBA system. The effect of dead zones on low viscosity particles in the WBA system is the observed in the velocity of the low viscosity particle at the late stage. However, dead zones do not decrease the average particle velocity in the DBA system. I believe that the strong liquid bridge force bonds in the DBA system is the cause. The particles in dead zones are dragged by other particles due to the liquid bridge. Collision frequency of high viscosity particle in WBA system is slightly higher than the particles in the DBA system. The hypothesis is that the larger granules formed in the

DBA systems reduce the collision frequency. However, DEM method tracks particles individually, the granule size is hard to be determined. Therefore, the average number of the liquid bridges on an API is considered as an indicator of the granule size. The DBA system possesses a higher average bridge number than the WBA system which supports our hypothesis. However, a more direct evidence is needed to justify it. Since the PBMs can compute the change in particle size distribution, a PBM-DEM coupled framework can be a future work to verify the hypothesis. Validation of our model is another thing can be done by the coupled framework since it's difficult to extract particle level information from experiment. Besides the PBM-DEM framework, consolidation is not considered in the simulation which leaves rooms for the improvement in our contact model.

References

[1] K. A. Mehta, G. S. Rekhi, and D. M. Parikh, “Handbook of Pharmaceutical Granulation Technology,” *Handb. Pharm. Granulation Technol.*, pp. 333–363, 2005.

[2] S. M. Iveson, J. D. Litster, K. Hapgood, and B. J. Ennis, “Nucleation, growth and breakage phenomena in agitated wet granulation processes: A review,” *Powder Technol.*, vol. 117, no. 1–2, pp. 3–39, 2001.

[3] R. Agrawal and Y. Naveen, “Pharmaceutical Processing – A Review on Wet Granulation Technology,” *Int. J. Pharm. Front. Res.*, vol. 1, no. June, pp. 65–83, 2011.

[4] H. Leuenberger, H and Bier, HP and Sucker, “Determination of the liquid requirement for a conventional granulation process,” *Ger Chem Eng*, vol. 4, pp. 13--18, 1981.

[5] R. C. Rowe and G. R. Sadeghnejad, “The rheology of microcrystalline cellulose powder/water mixes - measurement using a mixer torque rheometer,” *Int. J. Pharm.*, vol. 38, no. 1–3, pp. 227–229, 1987.

[6] K. V. S. Sastry and D. W. Fuerstenau, “Mechanisms of agglomerate growth in green pelletization,” *Powder Technol.*, vol. 7, no. 2, pp. 97–105, 1973.

[7] R. H. Perry, D. W. Green, and J. O. Maloney, “Perry’s chemical engineers’ handbook. 7th,” *McGrow-Hill, New York*, 1997.

[8] K. P. Hapgood, J. D. Litster, S. R. Biggs, and T. Howes, “Drop penetration into porous powder beds.,” *J. Colloid Interface Sci.*, vol. 253, no. 2, pp. 353–66, 2002.

[9] P. York and R. C. Rowe, “Monitoring granulation size enlargement process using mixer torque rheometry,” in *First International Particle Technology Forum, Denver, USA*, 1994.

[10] K. P. Hapgood, J. D. Litster, and R. Smith, “Nucleation regime map for liquid bound granules,” *AIChE J.*, vol. 49, no. 2, pp. 350–361, 2003.

[11] H. Rumpf and N. A. Knepper, “Agglomeration Interscience,” *New York*, 1962.

[12] K. Hotta, K. Takeda, and K. Iinoya, “The capillary binding force of a liquid bridge,” *Powder Technol.*, vol. 10, no. 4–5, pp. 231–242, 1974.

[13] G. Lian, C. Thornton, and M. J. Adams, “A theoretical study of the liquid bridge forces between two rigid spherical bodies,” *J. Colloid Interface Sci.*, vol. 161, no. 1, pp. 138–147, 1993.

[14] M. J. Adams and B. Edmondson, “Forces between particles in continuous and discrete liquid media,” *Tribol. Part. Technol.*, vol. 154, p. 172, 1987.

[15] D. N. Mazzone, G. I. Tardos, and R. Pfeffer, “The behavior of liquid bridges between two relatively moving particles,” *Powder Technol.*, vol. 51, no. 1, pp. 71–83, 1987.

[16] B. J. Ennis, J. Li, T. Gabriel I., and P. Robert, “The influence of viscosity on the strength of an axially strained pendular liquid bridge,” *Chem. Eng. Sci.*, vol. 45, no. 10, pp. 3071–3088, 1990.

[17] P. C. Kapur and D. W. Fuerstenau, “Coalescence model for granulation,” *Ind. Eng. Chem. Process Des. Dev.*, vol. 8, no. 1, pp. 56–62, 1969.

[18] B. J. Ennis, G. Tardos, and R. Pfeffer, “A microlevel-based characterization of granulation phenomena,” *Powder Technol.*, vol. 65, no. 1–3, pp. 257–272, 1991.

[19] L. Liu, J. Litster, S. Iveson, and B. Ennis, “Coalescence of deformable granules in wet granulation processes,” *AIChE J.*, vol. 46, no. 3, pp. 529–539, 2000.

[20] S. M. Iveson and J. D. Litster, “Growth regime map for liquid-bound granules,” *AIChE J.*, vol. 44, no. 7, pp. 1510–1518, 1998.

[21] G. K. Reynolds, J. S. Fu, Y. S. Cheong, M. J. Hounslow, and A. D. Salman, “Breakage in granulation: A review,” *Chem. Eng. Sci.*, vol. 60, no. 14, pp. 3969–3992, 2005.

[22] J. S. Ramaker, M. A. Jelgersma, P. Vonk, and N. W. F. Kossen, “Scale-down of a high-shear pelletisation process: Flow profile and growth kinetics,” *Int. J. Pharm.*, vol. 166, no. 1, pp. 89–97, 1998.

[23] G. I. Tardos, M. I. Khan, and P. R. Mort, “Critical parameters and limiting conditions in binder granulation of fine powders,” *Powder Technol.*, vol. 94, no. 3, pp. 245–258, 1997.

[24] J. Li, L. Tao, M. Dali, D. Buckley, J. Gao, and M. Hubert, “The Effect of the Physical States of Binders on High-Shear Wet Granulation and Granule Properties: A Mechanistic Approach Towards Understanding High-Shear Wet Granulation Process. Part I. Physical Characterization of Binders,” *J. Pharm. Sci.*, vol. 100, no. 1, pp. 164–173, 2011.

[25] A. Larsson, M. H. Vogt, J. Herder, and P. Luukkonen, “Novel mechanistic description of the water granulation process for hydrophilic polymers,” *Powder Technol.*, vol. 188, no. 2, pp. 139–146, 2008.

[26] M. Cavinato, M. Bresciani, M. Machin, G. Bellazzi, P. Canu, and A. C. Santomaso, “Formulation design for optimal high-shear wet granulation using on-line torque measurements,” *Int. J. Pharm.*, vol. 387, no. 1–2, pp. 48–55, 2010.

[27] D. Kayrak-Talay and J. D. Litster, “A priori performance prediction in pharmaceutical wet granulation: Testing the applicability of the nucleation regime map to a formulation with a broad size distribution and dry binder addition,” *Int. J. Pharm.*, vol. 418, no. 2, pp. 254–264, 2011.

[28] D. Barrasso and R. Ramachandran, “Multi-scale modeling of granulation processes: Bi-directional coupling of PBM with DEM via collision frequencies,” *Chem. Eng. Res. Des.*, vol. 93, no. April, pp. 304–317, 2015.

[29] M. J. Hounslow, “The Population Balance as a Tool for Understanding Particle Rate Processes,” *Kona*, vol. 16, no. 16, pp. 179–193, 1998.

[30] J. M.-H. Poon, C. D. Immanuel, F. J. Doyle Iii, and J. D. Litster, “A three-dimensional population balance model of granulation with a mechanistic representation of the nucleation and aggregation phenomena,” *Chem. Eng. Sci.*, vol. 63, no. 5, pp. 1315–1329, 2008.

[31] D. Barrasso and R. Ramachandran, “A comparison of model order reduction techniques for a four-dimensional population balance model describing multi-component wet granulation processes,” *Chem. Eng. Sci.*, vol. 80, pp. 380–392, 2012.

[32] T. Mikami, H. Kamiya, and M. Horio, “Numerical simulation of cohesive powder behavior in a fluidized bed,” *Chem. Eng. Sci.*, vol. 53, no. 10, pp. 1927–1940, 1998.

[33] G. Lian, C. Thornton, and M. J. Adams, “Discrete particle simulation of agglomerate impact coalescence,” *Chem. Eng. Sci.*, vol. 53, no. 19, pp. 3381–3391, 1998.

[34] B. Remy, B. J. Glasser, and J. G. Khinast, “The effect of mixer properties and fill level on granular flow in a bladed mixer,” *AIChE J.*, vol. 56, no. 2, pp. 336–353, 2010.

[35] J. A. Gantt, I. T. Cameron, J. D. Litster, and E. P. Gatzke, “Determination of coalescence kernels for high-shear granulation using DEM simulations,” *Powder Technol.*, vol. 170, no. 2, pp. 53–63, 2006.

[36] D. Barrasso, A. Tamrakar, and R. Ramachandran, “A reduced order PBM-ANN model of a multi-scale PBM-DEM description of a wet granulation process,” *Chem. Eng. Sci.*, vol. 119, pp. 319–329, 2014.

[37] M. Sen, D. Barrasso, R. Singh, and R. Ramachandran, “A Multi-Scale Hybrid CFD-DEM-PBM Description of a Fluid-Bed Granulation Process,” *Processes*, vol. 2, no. 1, pp. 89–111, 2014.

[38] S.Ardizzone *et al.*, “Microcrystalline cellulose powders: structure, surface features and water sorption capability,” *Cellulose*, vol. 6, pp. 57–69, 1999.

[39] M. J. Cliff and M. D. Parker, “Scale-up of mixer granulators,” in *Proceedings of the 12th Interphex Conference*, 1990, vol. 5, pp. 17–32.

[40] M. Landin, P. York, M. J. Cliff, R. C. Rowe, and A. J. Wigmore, “Scale-up of a pharmaceutical granulation in fixed bowl mixer-granulators,” *Int. J. Pharm.*, vol. 133, no. 1–2, pp. 127–131, 1996.

[41] P. Yadav and J. S. Chauhan, “A Review : On Scale-Up Factor Determination of Rapid Mixer,” *Sch. Res. Libr.*, vol. 2, no. 5, pp. 23–38, 2010.

[42] J. D. Litster, K. P. Hapgood, J. N. Michaels, A. Sims, M. Roberts, and S. K. Kameneni, “Scale-up of mixer granulators for effective liquid distribution,” *Powder Technol.*, vol. 124, no. 3, pp. 272–280, 2002.

[43] Y. Tsuji, T. Kawaguchi, and T. Tanaka, “Discrete particle simulation of two-dimensional fluidized bed,” *Powder Technol.*, vol. 77, no. 77, pp. 79–87, 1993.

[44] P. Lambert, A. Chau, A. D. Rgnier, and A. Delchambre, “Comparison between Two Capillary Forces Models Comparison between Two Capillary Forces Models,” vol. 24, no. 7, pp. 3157–3163, 2008.

[45] Y. I. Rabinovich, M. S. Esayanur, and B. M. Moudgil, “Capillary forces between two spheres with a fixed volume liquid bridge: Theory and experiment,” *Langmuir*, vol. 21, no. 24, pp. 10992–10997, 2005.

[46] P. Y. Liu, R. Y. Yang, and A. B. Yu, “Dynamics of wet particles in rotating drums: Effect of liquid surface tension,” *Phys. Fluids*, vol. 23, no. 1, 2011.

[47] K. Washino, K. Miyazaki, T. Tsuji, and T. Tanaka, “A new contact liquid dispersion model for discrete particle simulation,” *Chem. Eng. Res. Des.*, vol. 110, pp. 123–130, 2016.

[48] A. Anand, J. S. Curtis, C. R. Wassgren, B. C. Hancock, and W. R. Ketterhagen, “Predicting discharge dynamics of wet cohesive particles from a rectangular hopper using the discrete element method (DEM),” *Chem. Eng. Sci.*, vol. 64, no. 24, pp. 5268–5275,

2009.

[49] D. Shi and J. J. McCarthy, “Numerical simulation of liquid transfer between particles,” *Powder Technol.*, vol. 184, no. 1, pp. 64–75, 2008.

[50] A. J. Goldman, R. G. Cox, and H. Brenner, “Slow viscous motion of a sphere parallel to a plane wall - II Couette flow,” *Chem. Eng. Sci.*, vol. 22, no. 4, pp. 653–660, 1967.

[51] Ashland, “Klucel. Hydroxypropylcellulose. Physical and chemical properties,” p. www.aqualon.com, 2001.

[52] D. E. R. E. K. G. Gray, “The Surface Tension of Aqueous Hydroxypropyl Cellulose Solutions,” vol. 67, no. 2, pp. 255–265, 1978.

[53] S. Mezdour, G. Cuvelier, M. J. Cash, and C. Michon, “Surface rheological properties of hydroxypropyl cellulose at air-water interface,” *Food Hydrocoll.*, vol. 21, no. 5–6, pp. 776–781, 2007.

[54] a. H. Pelofsky, “Surface Tension-Viscosity Relation for Liquids.,” *J. Chem. Eng. Data*, vol. 11, no. 3, pp. 394–397, 1966.

[55] A. Siebold, A. Walliser, M. Nardin, M. Oppliger, and J. Schultz, “Capillary Rise for Thermodynamic Characterization of Solid Particle Surface,” *J. Colloid Interface Sci.*, vol. 186, no. 1, pp. 60–70, 1997.

[56] P. Luukkonen, T. Maloney, J. Rantanen, H. Paulapuro, and J. Yliruusi, “Interaction — A Novel Approach Using Thermoporosimetry,” *Pharm. Res.*, vol. 18, no. 11, pp. 1562–1569, 2001.

[57] P. C. Knight, T. Instone, J. M. K. Pearson, and M. J. Hounslow, “An investigation into the kinetics of liquid distribution and growth in high shear mixer agglomeration,” *Powder Technol.*, vol. 97, no. 3, pp. 246–257, 1998.